A novel temperature-controlled laser system to uniformly activate cutaneous thermal receptors during movable thermal stimulation

Rujoie, Ahmad; Andersen, Ole Kæseler; Frahm, Ken Steffen

Published in:
Journal of Neural Engineering

DOI (link to publication from Publisher):
10.1088/1741-2552/acb2f9

Publication date:
2023

Document Version
Accepted author manuscript, peer reviewed version

Accepted author manuscript of the article: Ahmad Rujoie et al 2023 J. Neural Eng. 20 016040. DOI: 10.1088/1741-2552/acb2f9

A novel temperature-controlled laser system to uniformly activate cutaneous thermal receptors during movable thermal stimulation

Ahmad Rujoie*, Ole Kæseler Andersen, Ken Steffen Frahm

Integrative Neuroscience group, Center for Neuroplasticity and Pain (CNAP), Department of Health Science & Technology, Aalborg University, Denmark

Abstract

Objective. Laser stimulators have been widely used in pain studies to selectively activate Aδ and C nociceptors without coactivation of mechanoreceptors. Temperature-controlled laser systems have been implemented with low-temperature variations during stimulations, however, these systems purely enabled stationary stimulation. This study aimed to implement, test and validate a new laser stimulation system that controls skin temperature by continuously adjusting laser output during stimulus movement to allow accurate investigation of tempo-spatial mechanisms in the nociceptive system. Approach. For validation, laser stimuli were delivered to the right forearm of eight healthy subjects using a diode laser. The laser beam was displaced across the skin to deliver a moving thermal stimulation to the skin surface. To test the function and feasibility of the system, different stimulation parameters were investigated involving two control modes (open-loop and closed-loop), three displacement velocities (5, 10 and 12 mm/s), two intensities (high 46 °C and low 42 °C), two stimulus lengths (20 and 100 mm) and two directions (distal and proximal). Main results. During closed-loop control, the stimulation error and variation of stimulation temperatures were significantly smaller than during open-loop control. The standard deviation of stimulation temperatures increased significantly with stimulation intensity and displacement length. Significance. This study showed that more accurate, less variable laser stimulations were delivered to the skin using closed-loop control during a movable stimulus. The more uniform skin temperature during stimuli is likely to ensure a more uniform nociceptor activation.

Keywords: laser stimulation, temperature-controlled system, diode laser, thermal receptor, nociceptive system, pain, healthy subjects

1. Introduction

In the somatosensory system, humans interact with the outer and inner world [1]. Receptors located in the periphery transduce external stimuli into action potentials that are conveyed to the central nervous system through sensory afferent fibers [1]. During research, when the purpose is to investigate the processing of neural information through the somatosensory systems, controlled stimuli are employed to activate those receptors [2]. In order to allow investigation of the nociceptive system, as a subsystem of the somatosensory system, which is responsible for transducing noxious stimuli to prevent tissue damage, the stimulation system needs to be able to deliver a stimulus of sufficient energy [3]. Further investigation of the nociceptive system is needed to get a better understanding of chronic pain and its mechanisms [3]. More than 30% of people worldwide are suffering from chronic pain [4] and the prevalence reasons for chronic pain are still unrevealed. Furthermore, one poorly understood mechanism is how temporal and spatial information are integrated in the nociceptive system. There is a lack of knowledge related to tempo-spatial mechanisms in the nociceptive system, hence to probe and understand these mechanisms, movable noxious stimuli are delivered to the skin [5]

Different stimulation modalities have been used to excite cutaneous nociceptors. The most commonly used stimulation modalities include mechanical, noxious heat, and noxious cold stimuli [2]. Mechanical stimuli are usually delivered by punctate stimuli or pressure algometers. Contact heat stimulation is applied using a thermode to allow precise temperature control but coactivation of mechanoreceptors as the probe is in contact with the skin [2]. Laser stimulators have been extensively utilized in animal and human pain studies [6][7] because of the ability to provide non-contact cutaneous stimulus allowing purely thermal stimulation. Additionally, laser stimulation eliminates stimulation artifacts and improves the spatial resolution of a stimulus [8]. Laser stimulation allows the selective activation of unmyelinated C and myelinated Aδ fiber nociceptors (creating a burning and pin-prick pain sensation) [9] and also non-nociceptive C fiber warmth afferents through radiant skin heating.

Different laser types have been employed to study the nociceptive system, e.g., argon ion [10][11], copper vapor [6][9], YAG (neodymium-YAG and thulium-YAG) [7], diode [12][13] and the most commonly used carbon dioxide (CO_2) laser [9][14]. The laser wavelength determines the absorption of laser photons, so the penetration depth is wavelength-dependent [15]. Compared to the CO_2 laser beam (wavelength: 10600 nm) [6], which is superficially absorbed up to 50 μm from the skin surface [16], the diode lasers beam, which radiating in the near-infrared region (wavelength: 800–980 nm) [17] penetrates deeper from 2 mm up to 2.5 mm into the human skin [18]. Since the nociceptors are not located at the skin surface [3], contact heat or low penetrating lasers (e.g., CO_2 laser) need passive conduction to allow the thermal energy to reach the nociceptors. Deeper penetration lasers, like a diode laser, allow more direct heating of the nociceptors and

eliminate the need for passive conduction [19]. Therefore, higher penetration lasers allow a more preferential activation of heat nociceptors without overheating the most superficial layers [19].

Several previous studies have used laser stimulation to investigate the nociceptive system [20][21][22][23]. The challenge of laser stimulation is to ensure uniform activation of the nociceptors. This is possible via assessment of skin temperature and active control of the laser power. Assessment of skin temperature is possible using a radiometer [24][25], infrared (IR) thermometer [26] or an IR camera [2][27]. Control of stimulation intensity has, in general, been implemented by an open-loop strategy, in which stimulation was delivered using a constant laser power for the duration of stimulation [27][28][29]. Such an open-loop approach is simple to implement, but it presents a major flaw. With this type of system, skin temperature is not controlled during the stimulation, instead laser power is set at the beginning and kept constant. To have low-temperature variations during the laser stimulation, closed-loop control systems have been implemented [24][25][30][31][32] that purely involved stationary stimuli. This type of control involves skin temperature feedback to adjust the laser power dynamically. Therefore, the actual skin temperature should remain closer to the desired temperature with less variation during the stimulation.

To investigate temporal and spatial mechanisms in the nociceptive system, a stimulation system is needed which allows displacement of the laser beam during stimulation [33]. Few studies have been published that involved a movable laser stimulus and they were all implemented using open-loop intensity control [27][33][34][5][35]. Therefore, there exist several limitations in our ability to investigate the tempo-spatial integration in the nociceptive system.

Therefore, the aim of this study was to implement, test and validate a new laser stimulation system that allows a movable cutaneous stimulation with closed-loop control of stimulus intensity to ensure uniform skin temperature. It was hypothesized that the use of a temperature-controlled stimulator system based on a closed-loop control strategy leads to more precise stimulation than open-loop control meaning lower variability in skin temperature during a moveable thermal stimulus. Furthermore, it was hypothesized that more uniform nociceptor activation results in a smaller perceptual variation.

2. Material and methods

2.1. System development

A 20 W, 970 nm diode laser (DL-20; IPG Laser, Burbach, Germany) with continuous-wave (CW) operation mode was used as the heat source to deliver the thermal stimuli (Fig. 1). An IR camera (FLIR SC645, Sweden) with a sampling frequency of 25 Hz was utilized to measure the skin temperature remotely. The

focusing lens of diode laser and IR camera were installed on a cartesian robot (TTA-A3G-30-30; Tabletop Robot, IAI, Shizuoka, Japan) to move the laser beam across the skin. The focusing lens (diameter: 20 mm) itself is made of glass and has a focal point at 20 mm where the beam is approx.4 mm, at 13 mm the beam diameter is approx. 5mm. The laser beam was kept perpendicular to the stimulation site throughout the stimulations. The distance between the focusing lens and the skin was kept constant at 13 cm, thus, ensuring that the laser beam had a diameter of 5 mm on the skin surface (this was confirmed by IR imaging). The stimulation control software was implemented in LabVIEW 21 (National Instruments, Austin, TX, USA) on a PC that communicated with the cartesian robot, IR camera and diode laser (Fig. 1).

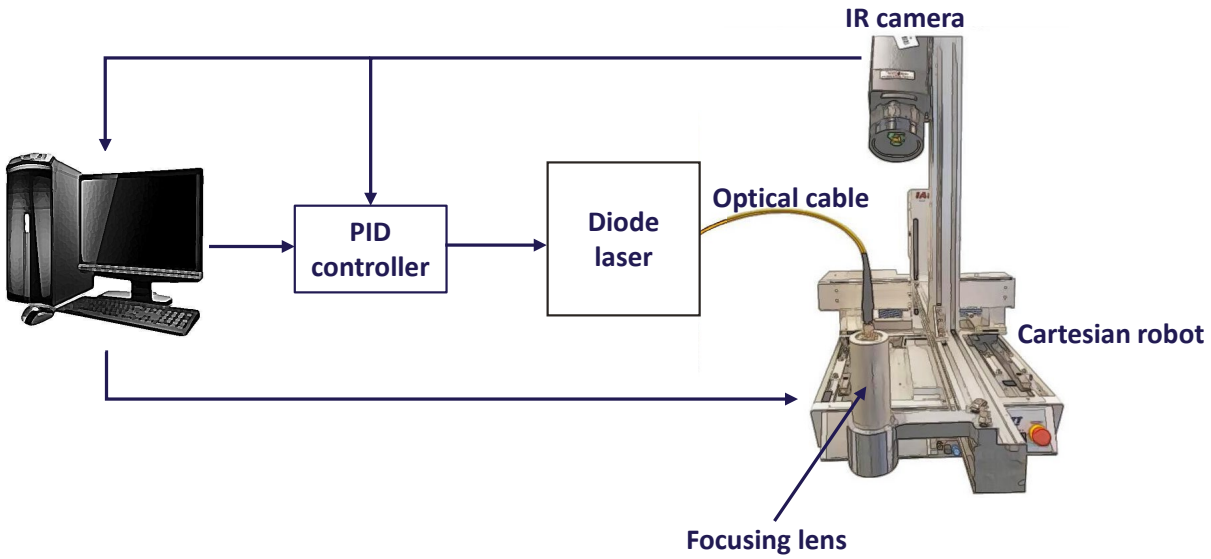

Figure 1. Schematic diagram of the stimulation system. Both IR camera and laser's focusing lens were installed on the cartesian robot to attain the movement ability. The distance of the IR camera and focusing lens was adjusted 40 cm and 13 cm from the stimulation area, respectively. The skin temperature was continuously measured by the IR camera and transferred to the computer to find and track the precise location of the laser beam on the skin. A proportional-integral-derivative (PID) controller regulated the power density based on temperature measurements provided by the IR camera.

2.1.1 Movement control

The cartesian robot can be moved and controlled in three directions (X, Y and Z-axis) with a movement accuracy of 0.01 mm. To ensure a steady, non-shaky movement during stimulation, the table movement was longer than the stimulation length (Fig. 2), i.e., the first and last 2 mm of the movement path was used for acceleration (ACC) and deceleration (DEC), respectively, without stimulation during these phases. The ACC and DEC were set to 0.1 G (1 G = 9800 mm/s^2).

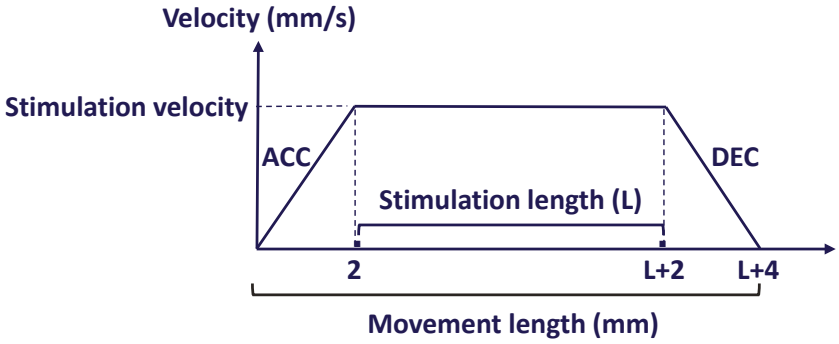

Figure 2. Schematic of the movement during stimulation. The movement path was longer than the actual stimulation length. To allow a steady movement, the ACC and DEC phases where not included in the stimulation length. The stimulation velocity was kept constant during each stimulation.

2.1.2. Temperature control

The closed-loop temperature control was based on a PID controller, adjusting the power density based on the temperature measurements from the IR camera. According to the image update frequency (25 Hz) and also to have sufficient computational time, the controller worked in 50 ms loops and the laser was turned on 49.5 ms in each loop (500 µs was allocated for communication with the diode laser). The PID gains were set for displacement velocities based on trial and error method (Table 1).

Table 1. The adjusted PID gains for different displacement velocities.

Velocity	PID gains		
	P	I	D
5 mm/s	0.14	0.005	0.35
10 mm/s	0.14	0.014	0.34
12 mm/s	0.14	0.016	0.34

To improve the temperature control during the start of the stimulation and to attain the fastest rise time, without increasing overshoot, an initial boost stimulation was used [24]. The purpose of the boost stimulation was to rapidly reduce the difference between the initial skin temperature and the target temperature. The boost consisted of a number of stimulation loops with maximum power density before enabling the PID controller (Fig. 3), i.e., a brief open-loop. The number of boost shots was determined

based on pilot experiments which set for each velocity and target stimulation intensity to ensure that boost made no overshoot (Table 2).

In order to compare closed-loop control to a simpler control scheme, an additional open-loop control mode was added as well. In open-loop control, the appropriate power density was adjusted individually for each subject, velocity and intensity meaning that before the experiment began, an initial estimate was tested during a small number of stimulations were applied on the same stimulation area and the power density was adjusted until the desired target temperature was reached. Then the stimulation power density was fixed for the remainder of the experiment.

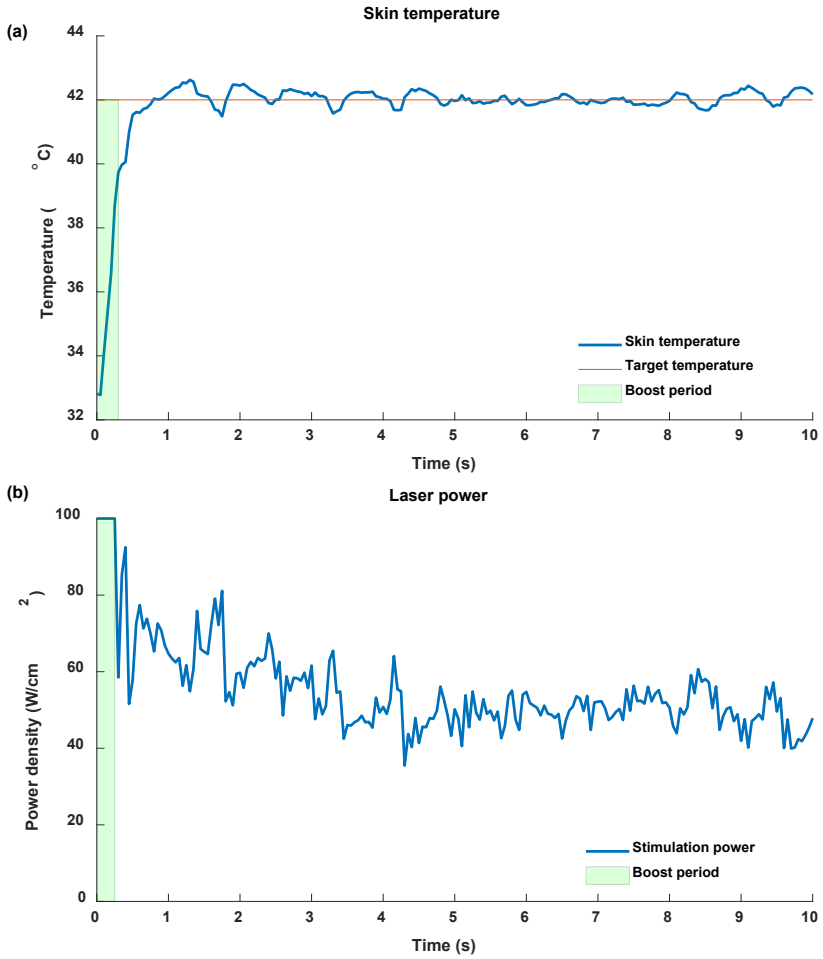

Figure 3. The system operation of closed-loop control during stimulation. a. The blue line indicates the highest temperature of the area where the laser spot was radiating on the skin and the red line represents the target temperature. b. The blue line shows the power density during stimulation. The green area demonstrates the boost period in which boost shots with maximum power density were delivered to the skin to decrease the rise time without making any overshoot. After the boost period, the PID controller was enabled to adjust the power density for the rest of the stimulation.

Table 2. The number of boost shots for different stimulation velocities and intensities.

Velocity	Target Intensity	
	Low (42 °C)	High (46 °C)
5 mm/s	2	3
10 mm/s	3	5
12 mm/s	4	6

2.1.3. Beam tracking

During the stimulation, the position of laser beam was not constant within the IR image frame because of small variations in the distance between the skin and the IR camera. Therefore, the exact location of the laser spot had to be found in each IR frame to provide feedback for the PID controller. The IR image was updated every 40 ms according to the sampling frequency of the IR camera (25 Hz). The IR image, with an image resolution of 640 × 480 pixels, was used to track the laser spot during the beam displacement (Fig. 4). The pixel size of the laser beam in the image depends on its distance and angle to the IR camera. Based on the distance between the camera and stimulation site (approx. 40 cm), the focusing lens and stimulation site (approx. 13 cm) and the angle between IR camera and laser beam (approx. 20 degrees) (Fig. 1) the laser beam projection on the skin represented q pixels, where q is the number of pixels which are occupied by the laser spot in the IR image. For a stationary laser stimulation, a fixed number of pixels can represent the laser spot because the distance between the focusing lens and stimulation area is the same during stimulation. However, during displaceable stimulation, because of the shape of body (e.g., forearm), the distance between the focusing lens and the stimulation area changes slightly (in the range of millimeters), which will result in small change in the number of pixels to represent the laser spot in the IR image. Hence, q pixels were considered to represent the location of laser spot in the thermographic image during the moveable stimulus. Practically, q was a number around 400. As mentioned, the camera and focusing lens were installed on the cartesian robot, so during the stimulation, their respective position to one another remained the same, although they were displaced across the skin. The location of laser spot was adjusted to be in the middle of the IR image in a stationary mode.

To locate the laser spot in the IR image during a moving stimulus, the basic idea was probing the whole thermographic image to find those pixels showing a temperature increase above a predefined threshold. A matrix method was designed to find the laser spot in the IR image during stimulation (Fig. 4). To decrease the computational load, a region of interest (ROI) with the size of m × n pixels was extracted from the IR image (Fig. 4). The laser stimulation increases the skin temperature, so the purpose of using the matrix

method was to find the pixels containing temperature increase due to the laser radiation. The location of the laser spot was found in each consecutive IR frame using the following algorithm:

1. Selecting two ROI matrices, one in the present frame and another being in frame x (Fig. 4), where frame x was one of the previous IR frames that was selected based on the movement velocity (Table 3). The present frame and frame x were used to compare the skin temperature at the current time and at 300 or 400 ms earlier than the current time, respectively. Frame x was determined to have a frame that had possible pixel representation, i.e., an integer value of pixel, of movement on the skin at each velocity.

2. Eliminating matrix rows/columns that are not available in both frames (making reduced ROI matrix in Fig. 4). Although the size of both ROI matrices was the same, because of the movement, the two ROI matrices were not located at the same place on the skin. Therefore, the non-overlapping parts of the two ROI matrices were removed. For instance, consider two simple matrices, $Y_1 = [y_1, y_2, y_3, y_4]$ regarding frame x and $Y_2 = [y_2, y_3, y_4, y_5]$ regarding the present frame, where y_i represents a specific location on the skin. The y_1 and y_5 pixels must be eliminated from the two ROI matrices to be at the same place on the skin, i.e. $[y_2, y_3, y_4]$, to compare the temperature development between frames. The number of rows/columns that moved for each velocity is shown in Table 3.

3. Subtracting the reduced ROI matrix in frame x (ROI_2) from the reduced ROI matrix in the present frame (ROI_1) to make the residual matrix (Fig. 4).

4. Finding q elements above a threshold in the residual matrix indicating the highest temperature difference. The temperature threshold of each velocity is shown in Table 3.

5. Identifying the found q pixels in the original ROI matrix of present frame as the laser beam location on the skin surface.

The maximum temperature value at the laser spot was used as feedback for the PID controller. The computation time of the matrix method was about 4 ms within each control loop.

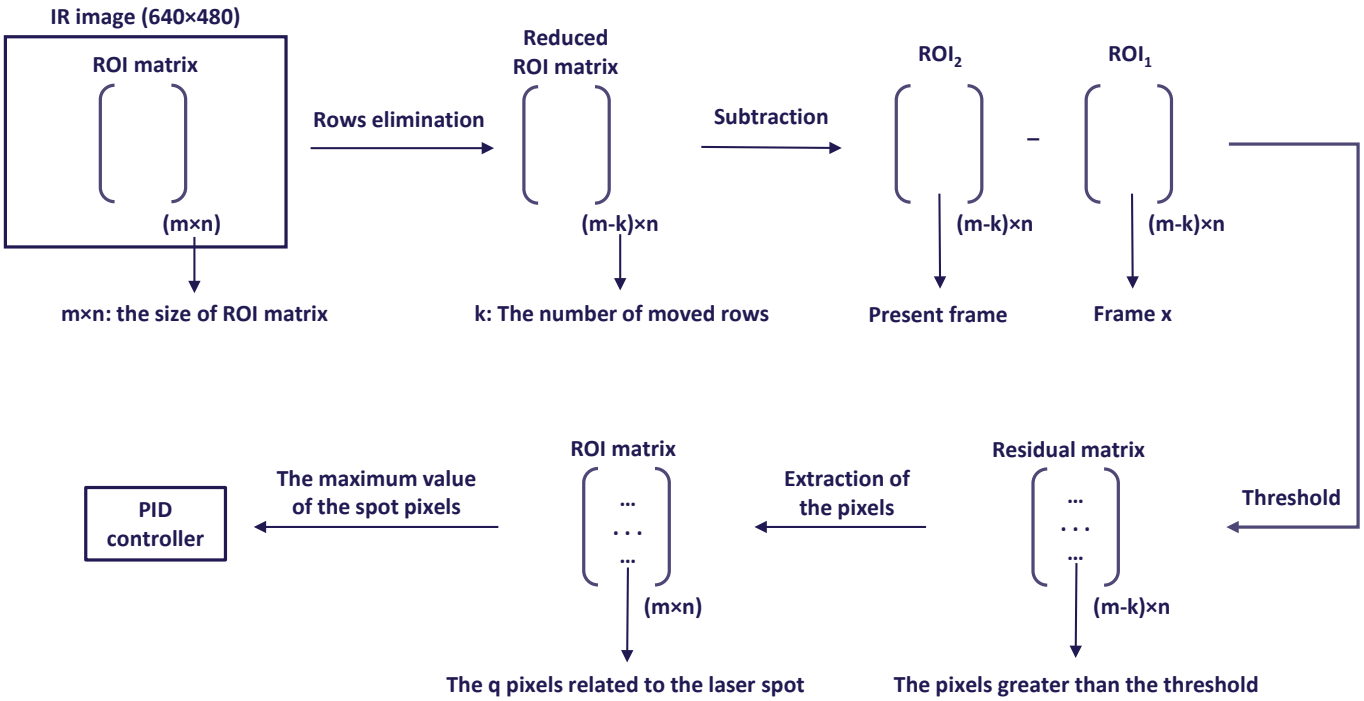

Figure 4. The designed matrix method to track the laser beam during stimulation. The ROI matrix is a sub-section of IR image, with the size of m×n in which m and n are the number of rows and columns, respectively, that contains the laser spot. The reduced ROI matrix is a sub-section of ROI, with the size of (m-k)×n, that is extracted based on the velocity of movement and k represents the number of moved rows in a specific number of IR frames. ROI_2 and ROI_1 signify the reduced ROI matrix in the present frame and in frame x, that frame x was presented in Table 3, respectively. The residual matrix was obtained by subtracting ROI_1 from ROI_2, and the q remainders above a threshold were related to the laser spot. By extracting these q pixels in the ROI matrix, the laser spot location was found as the location with peak temperature increase. The maximum temperature at the laser spot was used as feedback for the PID controller.

Table 3. The characteristic of the matrix method in each velocity.

Velocity (mm/s)	Frame x	The number of moved rows/columns	Threshold (°C)
5	Frame 8th prior to the present frame	5	0.3
10	Frame 6th prior to the present frame	8	0.4
12	Frame 8th prior to the present frame	11	0.4

2.2. System test and validation

2.2.1 Subjects

Eight healthy subjects (4 males, aged 26.6 ± 4.2 years) participated in the study. Seven of the subjects were Caucasian (4 males and 3 females) and one subject was Asian (female). The participants sat comfortably

in a chair during the experiment. Both subjects and the experimenter wore laser safety eye goggles. The laboratory temperature was 22 ℃ during the experiment. All participants gave written informed consent, according to the Declaration of Helsinki, prior to the experiment. The scientific ethics committee for region Nordjylland (North Denmark) approved all procedures of the experiment (ref. no. N-20200087).

2.2.2 Experimental protocol

To test the function and feasibility of the system, different stimulation parameters were investigated. The experiment consisted of two blocks, in each block either open-loop or closed-loop control was tested, and the order was randomized. In each block (Fig. 5), there were 48 stimulations, including three velocities (5, 10 and 12 mm/s), two intensities (high 46 ℃ and low 42 ℃), two displacement lengths (20 and 100 mm), two directions (distal and proximal) and two repetitions of each condition. In total, there were 96 stimulations (Fig. 5) and the order of stimulations was randomized inside each block.

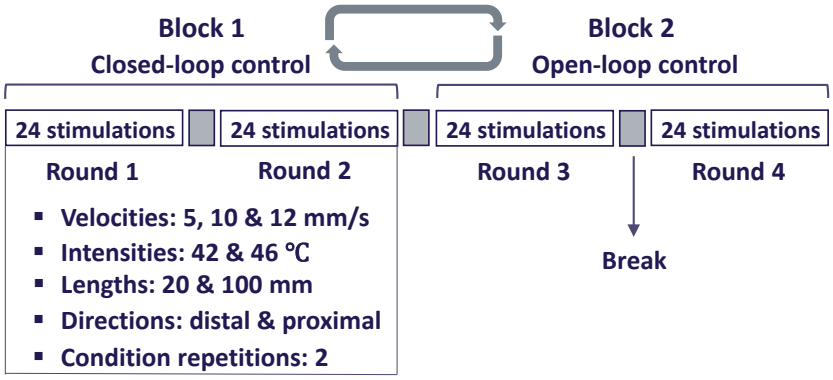

Figure 5. The experimental protocol. The experiment was performed in two blocks and each block was related to open/closed-loop control that consisted of 48 stimulations with different conditions (velocity, intensity, length, direction) and condition repetitions. Each block contained two stimulation rounds and a break between the rounds. The stimulations were delivered in randomized order.

The stimulation site was the right forearm and any hair growth on the volar forearm was removed before the experiment. The laser beam was continuously displaced across the skin distally or proximally to give a linear stimulation on the skin surface. The stimulation site was altered slightly between all stimuli. Prior to each stimulation, the IR recording was used to ensure that the skin area to be stimulated, had returned to baseline skin temperature. The laser was stopped if the skin temperature exceeded 50 ℃ during the stimulations. After each stimulation, the subjects were asked to rate the intensity of the pain perception on

a Numerical Rating Scale (NRS) anchored as 0 for no perception, 3 as pain threshold, and 10 as maximum imaginable pain.

2.2.3. Data analysis and statistics

The first 500 ms of each stimulation was considered as stimulus rise time, and results were analyzed after removing the rise time from all stimulations. The actual skin temperature during each stimulation frame (i.e., a 50 ms time frame that the laser was turned on) was extracted, based on matrix method (Fig. 4), and compared to the target temperature. The error was defined as the difference between the target and the actual temperature. The absolute error of stimulation temperature was obtained for the total stimulation time. The root mean squared error (RMSE) and standard deviation (SD) of temperatures were determined for all frames of each stimulation. The RMSE was used as a penalty function of stimulation error and the SD indicated the variability of stimulation temperatures. Differences in NRS, RMSE and SD of stimulation temperatures were analyzed using three linear mixed models (LMM). The control mode, velocity, displacement length, intensity and direction were used as fixed factors and the subject as random factor. P-values less than 0.05 were considered as significant. Data analysis was executed by MATLAB 2021 (The MathWorks, Inc., Natick, Massachusetts, USA).

3. Results

3.1. Temperature control

The absolute error was less than 1 ℃ for 90.4% of stimulus duration during closed-loop stimulations, but in open-loop control this was only the case in 47.3% of the stimulus duration of all stimulations (Fig. 6). Additionally, less than 3 % of closed-loop control had an error larger than 2 ℃, while this was the case in 18.9% in open-loop control (Fig. 6). The actual temperature of stimulation frames for different velocities, intensities and control modes are shown in Fig. 7 and Table 4. The average power density during stimulations is indicated in Table 5.

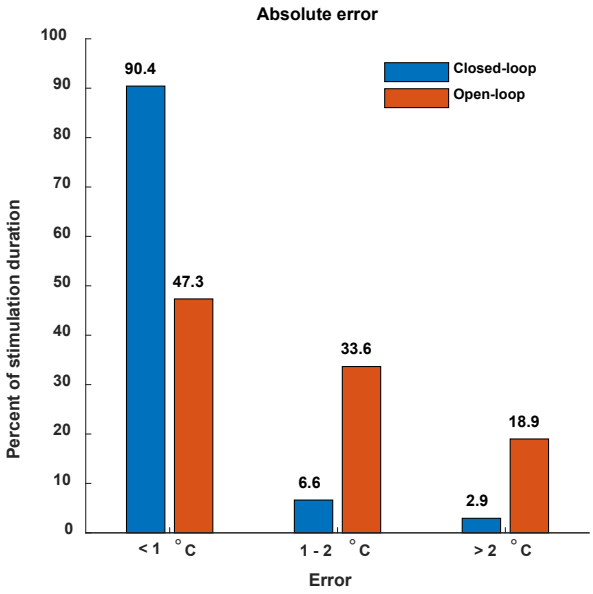

Figure 6. The absolute error distribution of stimulation temperature. The error was divided into three levels: less than 1 ℃, between 1 to 2 ℃ and greater than 2 ℃.

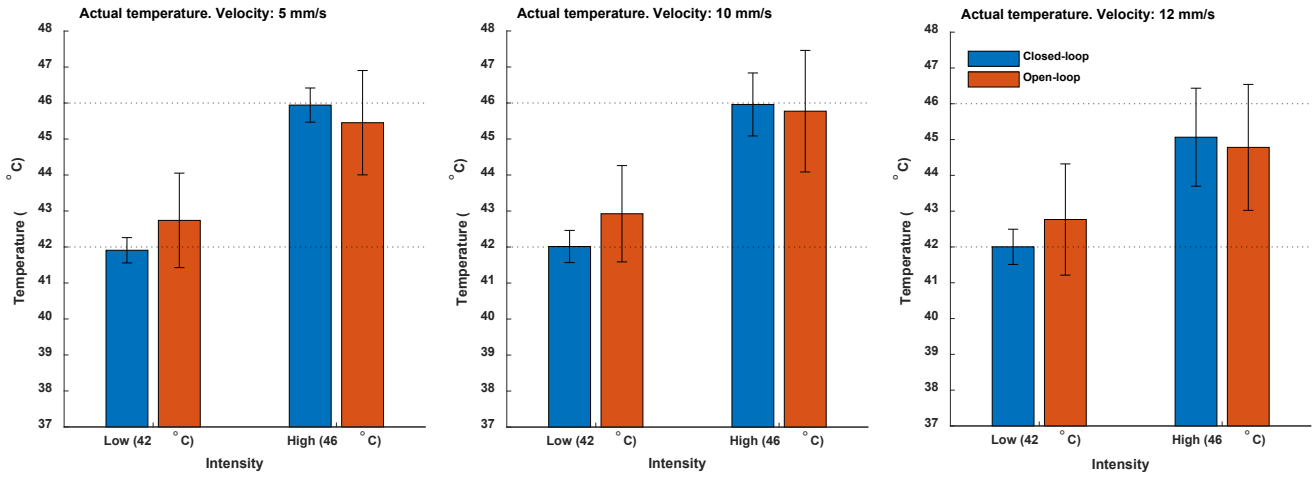

Figure 7. The average skin temperature during stimulations. Average values of actual temperature of whole stimulation frames across stimulation length for three velocities (left: 5 mm/s, middle: 10 mm/s, right: 12 mm/s), two intensities (low: 42 ℃, high: 46 ℃) and two control modes (open-loop, closed-loop control).

Table 4. The average skin temperature (℃) for different stimulation conditions.

Velocity	Open-loop control		Closed-loop control	
	Target intensity		Target intensity	
	Low (42 ℃)	High (46 ℃)	Low (42 ℃)	High (46 ℃)
5 mm/s	42.7 ± 1.3	45.4 ± 1.4	41.9 ± 0.3	45.9 ± 0.4

10 mm/s	42.9 ± 1.3	45.7 ± 1.6	42.0 ± 0.4	45.9 ± 0.8
12 mm/s	42.7 ± 1.5	44.7 ± 1.7	42.0 ± 0.4	45.0 ± 1.3

Table 5. The average power density (W/cm^2) of stimulations for different velocities, intensities and control modes.

Velocity	Open-loop control		Closed-loop control	
	Target intensity		Target intensity	
	Low (42 ℃)	High (46 ℃)	Low (42 ℃)	High (46 ℃)
5 mm/s	39.5 ± 1.0	48.0 ± 1.5	35.5 ± 7.5	48.0 ± 10.5
10 mm/s	65.0 ± 2.0	85.0 ± 2.0	59.5 ± 12.0	86.0 ± 13.5
12 mm/s	76.0 ± 3.0	99.5 ± 0.5	70.5 ± 15.0	98.0 ± 5.5

For the RMSE of stimulation temperature, there was a significant interaction between control type and velocity (LMM, p-value < 0.01) in which the RMSE increased with displacement velocity in closed-loop control (Fig. 8). Moreover, an interaction between control type and intensity was found so that the RMSE increased with stimulation intensity in closed-loop control (LMM, p-value < 0.05). During closed-loop control, the stimulation error was significantly smaller than during open-loop control (LMM, p-value < 0.001) (Fig. 8). No significant differences were found in RMSE in relation to displacement length (LMM, p-value = 0.91) or direction (LMM, p-value = 0.98).

For the SD of the stimulation temperature, there was a significant interaction between control type and velocity (LMM, p-value < 0.001) in which the SD increased with velocity in closed-loop control (Fig. 8). During closed-loop control, the SD of stimulation temperature was significantly smaller than during open-loop control (LMM, p-value < 0.001) (Fig. 8). The SD increased significantly with intensity (LMM, p-value < 0.001) and displacement length (LMM, p-value < 0.001). A significant difference was found between the SD and stimulation direction (LMM, p-value < 0.001).

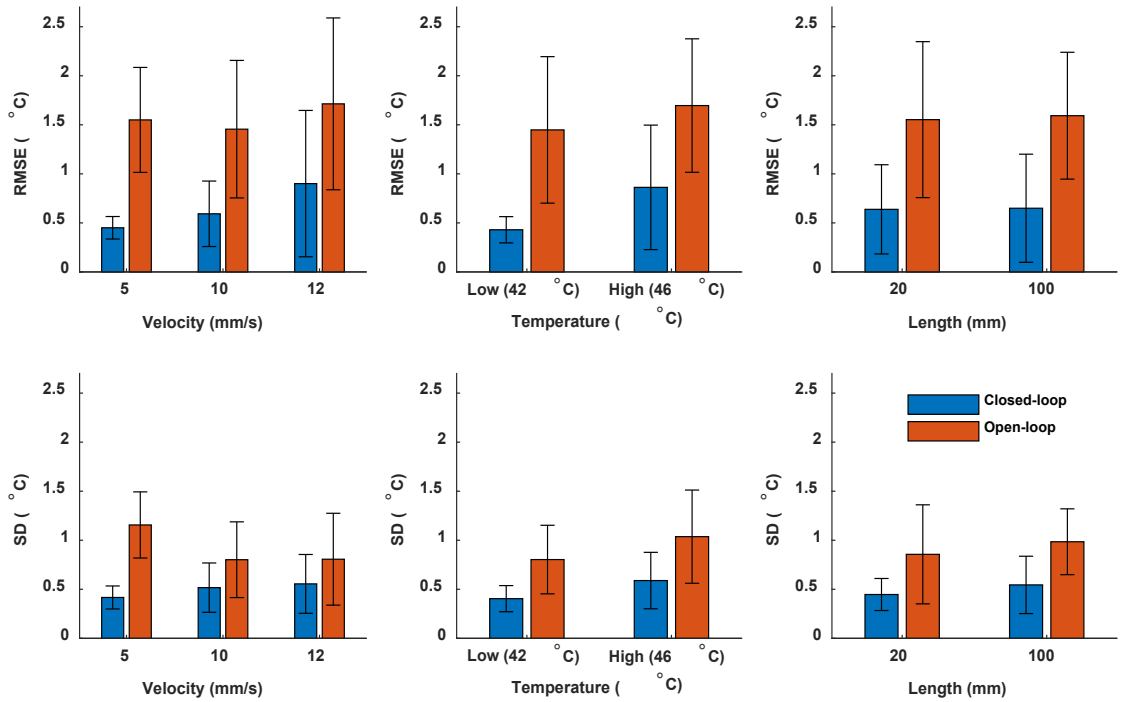

Figure 8. The error function (RMSE) (top) and SD (bottom) of the stimulation temperature in three velocities (left: 5 mm/s, 10 mm/s, 12 mm/s), two intensities (middle: 42 °C, 46 °C) and two lengths (right: 20 mm, 100 mm). The RMSE shows how accurate the stimulation temperatures are and the SD indicates how much the stimulation temperatures actually vary. In closed-loop control, the RMSE and SD increased with displacement velocity (LMM, p-value < 0.001) and stimulation intensity (LMM, p-value < 0.001). Both RMSE and SD decreased significantly during closed-loop control (LMM, p-value < 0.001).

3.2. Psycho-physical measures

The overall level and variance of the NRS increased significantly with the stimulation length (LMM, p-value < 0.001) and intensity (LMM, p-value < 0.001) (Fig. 9). During closed-loop control, the variance of the NRS was significantly smaller than during open-loop control (LMM, p-value < 0.001). In the distal direction, the NRS was significantly smaller than for the proximal direction (LMM, p-value < 0.01), but no significant difference was found between the NRS and stimulation velocity (LMM, p-value = 0.67).

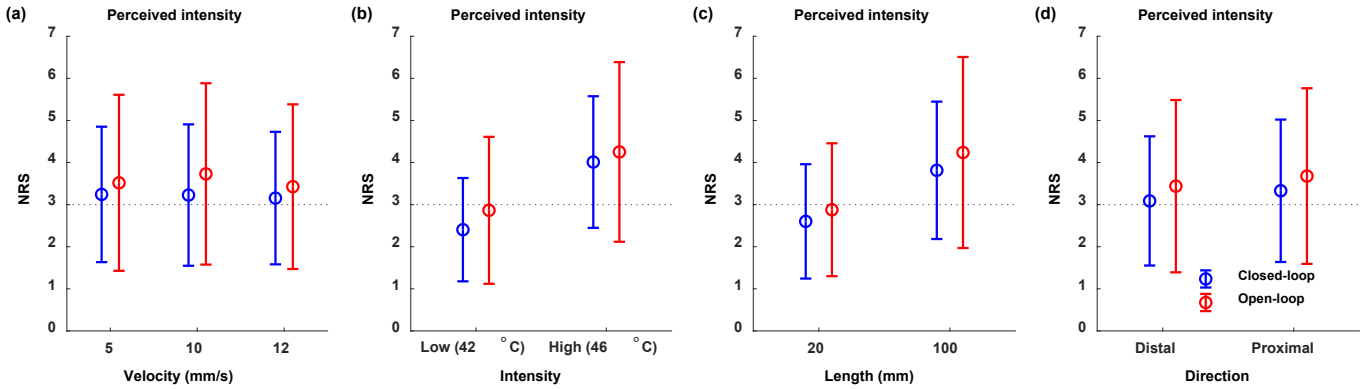

Figure 9. The NRS for different velocities (a), intensities (b), directions (c) and lengths (d). The dotted line indicates the pain perception. The figure shows how different stimulation conditions affect the perceived intensity on NRS. The NRS increased with stimulation intensity (LMM, p-value < 0.001) and displacement length (LMM, p-value < 0.001). The variance of NRS was significantly smaller during closed-loop control (LMM, p-value < 0.001).

4. Discussion

In the present study, a moveable temperature-controlled laser stimulation system was developed, tested and validated. The purpose of the new stimulator system was to decrease the variability and increase the accuracy of the temperature control during a moveable thermal stimulus and hence improve the precision of laser stimulation typically applied in studies of pain mechanisms. To validate the system performance, laser stimuli were delivered to healthy volunteers in different stimulation conditions, including three velocities, two intensities, two displacement lengths, two directions and two control modes. The experiments showed that the system delivers accurate temperature control during moveable cutaneous laser stimulation. Furthermore, when applying closed-loop temperature control, significantly more accurate and less variable stimulation temperature was achieved, as compared to open-loop control. Moreover, smaller variations of perceived intensities were observed when delivering closed-loop control stimulations.

4.1. Temperature control performance

The results of this study indicate that the absolute error during stimulation was less than 1 °C for the majority of the stimulation duration in closed-loop control (> 90 %), compared to less than half of the stimulation duration in open-loop control (Fig. 6). Furthermore, during closed-loop control, less than 3% of stimulation duration had an absolute error greater than 2 °C, compared to over 18% during open-loop control. Table 4 and Fig. 7 demonstrate that during closed-loop control, the average stimulation temperature was closer to the target temperature for all conditions compared to open-loop control, except for the velocity of 12 mm/s at the intensity of 46 °C that system was suffering to achieve the desired temperature, which is discussed below. Another important finding was that during closed-loop control, the stimulation error and the SD of

stimulation temperatures were significantly smaller than during open-loop control (Fig. 8), indicating that the overall performance of the system was substantially better in terms of temperature control.

In the mid-seventies, the first temperature-controlled laser stimulation system was implemented using a 50 W, 10.6 μm CO_2 laser as the heat source, a radiometer as a temperature sensor and control electronics as a feedback controller to deliver stationary stimuli to the skin [24]. In that study, a 10 ℃ temperature pulse, i.e., 10 ℃ increment of skin temperature compared to the baseline temperature, lasting 3 s, was delivered to the fingertip using a 7.5 mm diameter spot. The pulse rise time was below 0.3 ℃, and the average pulse temperature was reported 10 ± 0.1 ℃ at the skin surface. Additionally, the temperature was measured at different depths of skin from 100 to 700 μm and showed that the temperature decreased below a depth of 100 μm, indicating that this closed-loop control system precisely worked at the skin surface (a depth less than 100 μm), due to stimulation given by a CO_2 laser having low penetration. Although the accuracy of that system is better than the system used in the present study, it should be considered that our system controlled the skin temperature during beam displacement, and not only during stationary stimuli as done in [24]. When there is no beam displacement during stimulation, the temperature sensing is limited to a small and well-defined area on the skin surface. But conversely, when stimulating different cutaneous areas during beam movement across the skin, there is a major challenge as the thermo-dynamic system will vary during stimulation. For example, variation in size and density of hair follicles [36] and skin tone are likely to result in temperature changes during laser radiation as the photon absorption differs [37]. The current study showed that during the slow displacement velocity (5 mm/s), the rise time was below 0.4 s and the average skin temperature was 41.9 ± 0.3 ℃ for the low intensity and 45.9 ± 0.4 ℃ for the high intensity (Table 4) that indicating small variation of skin temperature, even though during movement.

Additionally, there were only very few studies in the literature that compared both open-loop and closed-loop laser stimulation systems. One example, however, was a study where in vitro, stationary stimulations were delivered to pieces of fresh pig skin using a 1940 nm Tm:YAG laser [32], in which closed-loop control (PID controller) was used to maintain the stimulation temperature between 50 and 55 ℃, and in open-loop control, constant power of 1.5 W was used during 5 min laser stimulation for both control modes. Their results showed that in closed-loop control, the mean temperature was 53.7 ± 1.3 ℃ with a temperature variation of 1.6 ± 0.2%, and a continuous temperature increment was observed during open-loop control with a final temperature up to 60 ℃ at the end of stimulation. Similar to the findings of the current study, their results showed that temperature control is superior during closed-loop control. Additionally, it must be noted that [32] used temperature control during stationary stimulations, which lasted a relatively long stimulation time (5 min) and their target temperatures were not a single fixed point, but a simply larger range between 50 ℃ and 55 ℃. In contrast, in the present study, movable stimulations were delivered to

the human skin in vivo to attain fixed target temperatures (42 ℃ and 46 ℃) with different and relatively shorter stimulation durations (1.66 - 20 s), because of using different displacement lengths and velocities, that entirely achieved better performance than what was reported in [32] in terms of temperature control for all stimulation conditions (Fig. 7 and Table 4).

In addition to delivering laser stimulations in vitro, invasive stationary laser stimulations including temperature control have been applied to the rat prostate cavernous nerves in vivo [30]. Those stimuli lasted 15-30 s, and were made using a 150 mW, 1455 nm diode laser with 1 mm diameter spot and an IR radiometer was used as a thermal sensor [30]. In that study, 94 mW constant power was set for open-loop control, and there were four different stimulation intensities for closed-loop control, including 42 ℃, 44 ℃, 46 ℃ and 48 ℃. Their results showed a continuous increment of nerve temperature up to 49 ℃ in open-loop control and the observed deviation from the set point value was ± 1 ℃ during closed-loop control. Real-time temperature control laser systems have also been employed for photothermal tissue welding (PTW) in surgeries [38][39] to prevent tissue injuries and also to maintain the tissue surface (TS) at the desired temperature during surgery. Rat aortas were welded using 1.9 μm diode laser with 0.7 mm spot to control TS temperature at 80 ℃, which after approx. 1 s as rise time, the surface temperature was maintained at 80 ± 2 ℃ during 5-8 s of temperature-controlled welding [38]. Moreover, in open-loop control, after 2 s as rise time, the surgeon could maintain TS temperature at 78 ± 5 ℃ during the weld. Another study employed temperature-controlled photocoagulation (TCPC) system, which consisted of a 1.32 μm Nd:YAG laser, an IR thermometer and a microprocessor as feedback controller [39]. In this study, pig tissue welding was performed in vivo using both open-loop and TCPC systems to have 20 s laser-welded repairs at 65 ℃, 75 ℃, 85 ℃ and 95 ℃. Their results indicated a variation of TS temperature between 70 ℃ and 100 ℃ during the open-loop weld, and the observed deviation for set point temperature was ± 4 ℃ using closed-loop control welding. Thus, [38][39] showed superior temperature control using closed-loop compared to open-loop, which are further supporting the findings of the current study. However, our temperature-controlled stimulation system, which worked during movement, had a short rise time (below 500 ms), and the overall level of temperature deviation was smaller than the achieved results of invasive stimulations in [38][39] for different stimulation conditions (Table 4).

4.2. Psycho-physical responses during stimulation

The results of this study indicate that during closed-loop control, the variance of the perceiving intensity (NRS) was significantly smaller than during open-loop control (Fig. 9). These psycho-physical results are in accordance with the stimulation temperature during closed-loop control, where the skin temperature variation was smaller than during open-loop control (Fig. 8). These findings indicate that the system is able to activate the cutaneous sensory receptors more uniformly and more reliably during closed-loop control,

and this supports the hypothesis that improved control of the stimulation temperature will give less variable perception intensity.

One interesting finding is that the NRS increased with displacement length (Fig. 9), which fits the results from previous studies using a movable laser stimulus [33][35]. This enhancement of perceived pain is likely caused by a larger stimulation area which will recruit more neurons, resulting in a spatial summation of pain [40][41][42]. Surprisingly Fig. 9 indicates there was no relation between the perceived intensity (NRS) and stimulation velocity. This finding is in contrast to a previous study by our group, which showed that the reported NRS decreased with increasing stimulation velocity [35]. It should be noted that our previous study used a CO_2 laser, and as mentioned before, the penetration by the CO_2 laser is very superficial (from 30 to 50 μm from the skin surface [16]) as most of its energy is absorbed by water within epidermis [43][11], and hence the produced heat is passively conducted to the receptor terminals located deeper in the skin [44]. The previous study used computational modeling to show that the temperature, where the receptors are located, was lower for faster stimulation velocities, caused by the lower penetration of the CO_2 stimuli [45], creating a discrepancy between surface and receptor temperature which is exacerbated for higher velocities. These lower temperatures at the nerve terminals are likely the cause for the lower reported NRS in [35]. This is in contrast to the current study, where a high penetrating laser was used as the stimulator. Due to the higher penetration of diode laser, there is little discrepancy between surface and receptor temperature [46]. This ensures that the receptor temperature does not depend on the stimulation velocity, and thus creating a more direct receptor activation without the need for passive heat conduction. Although the thermal sensors measure the skin surface temperature, the temperature at receptor level is close to the surface temperature as the absorption is more uniform using deep penetration lasers (e.g., solid-state and diode lasers) [46].

4.3. System limitation

In this study, there was a limitation in reaching the higher temperature target during the fastest velocity (12mm/s). For the velocity of 12 mm/s, during closed-loop control and low intensity, the target temperature was also reached, but for the high intensity, the system was close to unable to achieve the target temperature (Fig. 7 and Table 4). The reason for this error is likely that the diode laser had insufficient power to reach the noxious range (46 °C) for the velocity of 12 mm/s. For the velocity of 12 mm/s and high intensity, the average laser power was 19.6 ± 1.1 W during closed-loop and 19.9 ± 0.1 W during open-loop control, which is indeed very close to the maximum power of 20 W, but none of the control paradigms managed to reach the target temperature (Fig. 7). This also affected the overall performance of stimulations, i.e., the absolute error was less than that showed in Fig. 6 if the system had a more powerful diode laser. Therefore, for the present laser stimulator system, 10 mm/s should be the maximum beam displacement velocity for future

studies, if noxious temperatures are to be used. A potential future improvement of our system could be the usage of a more powerful diode laser, this would allow faster noxious stimuli. Additionally, a more powerful laser may allow fewer initial boost shots and have a faster rise time at the beginning of stimulations (Fig. 3).

5. Conclusion

To our knowledge, this is the first study describing a system that allows moveable, closed-loop temperature-controlled laser stimuli. The purpose of the system is to allow the investigation of temporal and spatial integration of nociceptive information using noxious laser stimulation. The system was developed, tested, and validated across different stimulation velocities, stimulation intensities, displacement lengths and directions. Closed-loop temperature control was shown to be associated with more accurate, less variable skin temperature and, perhaps more importantly, less variable psycho-physical recordings (NRS), indicating a more uniform nociceptor activation across subjects. The system will allow the investigation of the combined spatial and temporal integration of sensory information within the somatosensory system, and particularly the nociceptive system.

Acknowledgment:

The authors have no conflict of interest to declare. This study was funded by the Danish National Research Foundation (DNRF121).

References:

[1] Tibbetts P E 2013 Principles of Neural Science . Fifth Edition. Edited by Eric R. Kandel, James H. Schwartz, Thomas M. Jessell, Steven A. Siegelbaum, and A. J. Hudspeth; Art Editor:, Sarah Mack. New York: McGraw-Hill. $135.00. l + 1709 p.; ill.; index. ISBN: 978-0-07-1390 *Q. Rev. Biol.* **88** 139–40

[2] Plaghki L and Mouraux A 2003 How do we selectively activate skin nociceptors with a high power infrared laser? Physiology and biophysics of laser stimulation *Neurophysiol. Clin.* **33** 269–77

[3] Rathmell J P and Hill B 2006 Wall and Melzack's Textbook of Pain, 5th E-dition. *Anesth. Analg.* **102** 1914

[4] Cohen S P, Vase L and Hooten W M 2021 Chronic pain: an update on burden, best practices, and new advances *Lancet* **397** 2082–97

[5] Frahm K S, Mørch C D and Andersen O K 2019 Cutaneous nociceptive sensitization affects the directional discrimination-but not the 2-point discrimination *Scand. J. Pain* **19** 605–13

[6] Clark S, Dickinson M R, King T A, Jones A, Chen A, Derbyshire S, Townsend D W, Kinahan P E, Mintun M A and Nichols T 1996 Laser stimulation for pain research *Biomed. Optoelectron. Clin. Chem. Biotechnol.* **2629** 197–205

[7] Arendt-Nielsen L and Chen A C N 2003 Lasers and other thermal stimulators for activation of skin nociceptors in humans *Neurophysiol. Clin.* **33** 259–68

[8] Wells J D, M.D. C K, Jansen E D, M.D. P E K and Mahadevan-Jansen A 2005 Application of infrared light for in vivo neural stimulation *J. Biomed. Opt.* **10** 064003

[9] Svensson P, Bjerring P, Arendt-Nielsen L, Nielsen J C and Kaaber S 1991 Comparison of four laser types for experimental pain stimulation on oral mucosa and hairy skin *Lasers Surg. Med.* **11** 313–24

[10] Arendt-Nelsen L and Bjerring P 1988 Reaction times to painless and painful CO2 and argon laser stimulation *Eur. J. Appl. Physiol. Occup. Physiol.* **58** 266–73

[11] Arendt-Nielsen L and Bjerring P 1988 Sensory and pain threshold characteristics to laser stimuli *J. Neurol. Neurosurg. Psychiatry* **51** 35–42

[12] Gülsoy M, Durak K, Kurt A, Karamürsel S and Çilesiz I 2001 The 980-nm diode laser as a new stimulant for laser evoked potentials studies *Lasers Surg. Med.* **28** 244–7

[13] Greffrath W, Nemenov M I, Schwarz S, Baumgärtner U, Vogel H, Arendt-Nielsen L and Treede R D 2002 Inward currents in primary nociceptive neurons of the rat and pain sensations in humans elicited by infrared diode laser pulses *Pain* **99** 145–55

[14] McCaughey R, Nadeau V and Dickinson M 2005 Flat-top beam for laser-stimulated pain *Thermal Treatment of Tissue: Energy Delivery and Assessment III* vol 5698 p 263

[15] Boulnois J L 1986 Photophysical processes in recent medical laser developments: A review *Lasers Med. Sci. 1986 11* **1** 47–66

[16] Trelles M A, David L M and Rigau J 1996 Penetration Depth of Ultrapulse Carbon Dioxide Laser in Human Skin *Dermatologic Surg.* **22** 863–5

[17] Gülsoy M, Çelikel T, Kurtkaya Ö, Sav A, Kurt A, Canbeyli R and Çilesiz I 1999 Application of the

980-nm diode laser in sterotaxic surgery *IEEE J. Sel. Top. Quantum Electron.* **5** 1090–4

[18] Bashkatov A N, Genina E A, Kochubey V I and Tuchin V V. 2005 Optical properties of human skin, subcutaneous and mucous tissues in the wavelength range from 400 to 2000 nm *J. Phys. D. Appl. Phys.* **38** 2543

[19] Tzabazis A Z, Klukinov M, Crottaz-Herbette S, Nemenov M I, Angst M S and Yeomans D C 2011 Selective nociceptor activation in volunteers by infrared diode laser *Mol. Pain* **7** 1744–8069

[20] Moore C E G and Schady W 1995 Cutaneous localisation of laser induced pain in humans *Neurosci. Lett.* **193** 208–10

[21] Schlereth T, Magerl W and Treede R D 2001 Spatial discrimination thresholds for pain and touch in human hairy skin *Pain* **92** 187–94

[22] Martikainen I K and Pertovaara A 2002 Spatial discrimination of one versus two test stimuli in the human skin: Dissociation of mechanisms depending on the task and the modality of stimulation *Neurosci. Lett.* **328** 322–4

[23] Mancini F, Bauleo A, Cole J, Lui F, Porro C A, Haggard P and Iannetti G D 2014 Whole-body mapping of spatial acuity for pain and touch *Ann. Neurol.* **75** 917–24

[24] Meyer R A, Walker R E and Mountcastle V B 1976 A Laser Stimulator for the Study of Cutaneous Thermal and Pain Sensations *IEEE Trans. Biomed. Eng.* **BME-23** 54–60

[25] Wu G, Campbell J N and Meyer R A 2001 Effects of baseline skin temperature on pain ratings to suprathreshold temperature-controlled stimuli *Pain* **90** 151–6

[26] Iannetti G D, Zambreanu L and Tracey I 2006 Similar nociceptive afferents mediate psychophysical and electrophysiological responses to heat stimulation of glabrous and hairy skin in humans *J. Physiol.* **577** 235–48

[27] Mørch C D, Andersen O K, Quevedo A S, Arendt-Nielsen L and Coghill R C 2010 Exteroceptive aspects of nociception: Insights from graphesthesia and two-point discrimination *Pain* **151** 45–52

[28] Frahm K S, Gervasio S, Arguissain F and Mouraux A 2020 New Insights into Cutaneous Laser Stimulation – Dependency on Skin and Laser Type *Neuroscience* **448** 71–84

[29] Moeller-Bertram T, Schilling J M, Bačkonja M M and Nemenov M I 2013 Sensory small fiber function differentially assessed with diode laser (DL) quantitative sensory testing (QST) in painful neuropathy (PN) *Pain Med. (United States)* **14** 417–21

[30] Tozburun S, Hutchens T C, McClain M A, Lagoda G A, M.D. A L B and Fried N M 2013 Temperature-controlled optical stimulation of the rat prostate cavernous nerves *J. Biomed. Opt.* **18** 067001

[31] Marchandise E, Mouraux A, Plaghki L and Henrotte F 2014 Finite element analysis of thermal laser skin stimulation for a finer characterization of the nociceptive system *J. Neurosci. Methods* **223** 1–10

[32] Dong X, Liu T, Wang H, Yang J, Chen Z, Hu Y and Li Y 2017 A novel dual-wavelength laser stimulator to elicit transient and tonic nociceptive stimulation *Lasers Med. Sci.* **32** 1001–8

[33] Frahm K S, Mørch C D and Andersen O K 2018 Tempo-spatial discrimination is lower for noxious stimuli than for innocuous stimuli *Pain* **159** 393–401

[34] Quevedo A S, Mørch C D, Andersen O K and Coghill R C 2017 Lateral inhibition during nociceptive processing *Pain* **158** 1046–52

[35] Frahm K S, Mørch C D and Andersen O K 2020 Directional discrimination is better for noxious laser stimuli than for innocuous laser stimuli *Eur. J. Pain (United Kingdom)* **24** 742–51

[36] Otberg N, Richter H, Schaefer H, Blume-Peytavi U, Sterry W and Lademann J 2004 Variations of Hair Follicle Size and Distribution in Different Body Sites *J. Invest. Dermatol.* **122** 14–9

[37] Patil U and Dhami L 2008 Overview of lasers *Indian J. Plast. Surg.* **41** 101–13

[38] Stewart R B, Benbrahim A, Lamuraglia G M, Rosenberg M, L'ltalien G J, Abbott W M and Kung R T V 1996 Laser Assisted Vascular Welding With Real Time Temperature Control *Lasers Surg. Med.* **199**

[39] Poppas D P, Stewart R B, Mathieu Massicotte J, Wolga A E, Kung R T V, Retik A B and Freeman M R 1996 Temperature-controlled laser photocoagulation of soft tissue: In vivo evaluation using a tissue welding model *Lasers Surg. Med.* **18** 335–44

[40] Price D D, McHaffie J G and Larson M A 1989 Spatial summation of heat-induced pain: Influence of stimulus area and spatial separation of stimuli on perceived pain sensation intensity and unpleasantness *J. Neurophysiol.* **62** 1270–9

[41] Marchand S and Arsenault P 2002 Spatial summation for pain perception: Interaction of inhibitory and excitatory mechanisms *Pain* **95** 201–6

[42] Quevedo A S and Coghill R C 2009 Filling-in, spatial summation, and radiation of pain: Evidence

for a neural population code in the nociceptive system *J. Neurophysiol.* **102** 3544–53

[43] Brugmans M J P, Kemper J, Gijsbers G H M, van der Meulen F W and van Gemert M J C 1991 Temperature response of biological materials to pulsed non-ablative CO2 laser irradiation *Lasers Surg. Med.* **11** 587–94

[44] Bargeron C B, McCally R L and Farrell R A 1981 Calculated and measured endothelial temperature histories of excised rabbit corneas exposed to infrared radiation *Exp. Eye Res.* **32** 241–50

[45] Frahm K S, Andersen O K, Arendt-Nielsen L and Mørch C D 2010 Spatial temperature distribution in human hairy and glabrous skin after infrared CO2laser radiation *Biomed. Eng. Online* **9** 1–18

[46] Mørch C D, Frahm K S, Coghill R C, Arendt-Nielsen L and Andersen O K 2015 Distinct temporal filtering mechanisms are engaged during dynamic increases and decreases of noxious stimulus intensity *Pain* **156** 1906–12